SIGNAL-BASED INSTABILITY MONITORING OF ELECTRIC POWER SYSTEMS

Munther A. Hassouneh, Mohamed S. Saad and Eyad H. Abed

Department of Electrical and Computer Engineering and the Institute for Systems Research
University of Maryland, College Park, MD 20742, USA
munther@umd.edu mssaad@umd.edu abed@umd.edu

Abstract: Today's electric power systems are often subject to stress by heavy loading conditions, resulting in operation with a small margin of stability. This has led to research on estimating the distance to instability. Most of these research efforts are solely model-based. In this work, a signal-based approach for real-time detection of impending instability is considered. The main idea pursued here involves using a small additive white Gaussian noise as a probe signal and monitoring the spectral density of one or more measured states for certain signatures of impending instability. Input-to-state participation factors are introduced as a tool to aid in selection of locations for probe inputs and outputs to be monitored. Since these participation factors are model-based, the paper combines signal-based and model-based ideas toward achieving a robust methodology for instability monitoring.

Keywords: Monitoring, power systems, stability, instability, precursors, bifurcation, voltage collapse, participation factors.

1. INTRODUCTION

Today's electric power systems are often subject to stress due to heavy loading conditions. Under such conditions, a power system that appears to be functioning well could actually be very vulnerable to loss of stability. Stability loss can, in turn, trigger a chain of events leading to failure of the system. Stability loss can occur in several forms, but the most common one resulting from heavy load conditions is voltage instability, which leads to voltage collapse through cascading of system events (van Cutsem, 2000). This differs markedly from transient instability following a system contingency, since this type of instability usually results from slow changes in system parameters, such as loading or generation. There is an inherent difficulty in predicting voltage instability, since the parameter values at which it occurs depend on component dynamics in an uncertain and complex interconnected system. Inaccurate system models can easily yield incorrect results for the stability envelope of the system. When a system must be operated near its stability limits, any model uncertainty can result in the system exiting its stable operating regime without warning. Even the most detailed calculations are insufficient in these circumstances.

In this paper, instability monitoring using (noisy) probe signals is considered. The use of probe signals is shown to help reveal an impending loss of stability. This is because probe signals propagate in the power system and give certain signatures near an instability that can be used as a warning signal for possible impending voltage collapse. Such warning signals are needed to alert system operators of a situation that may require

preventive control, and to provide the operators with valuable additional time to take necessary preventive (rather than corrective) measures.

The paper proceeds as follows. In Section 2, participation factors for linear systems are discussed. This includes both the modal participation factors, and newly introduced input-to-state participation factors. In Section 3, a signal-based approach to instability monitoring is presented. In Section 4, a stability index based on power spectral density measurements is given. In Section 5, two case studies are given that demonstrate the proposed approach to instability monitoring.

2. PARTICIPATION FACTORS

Participation factors are nondimensional scalars that measure the interaction between the modes and the state variables of a linear system (Perez-Arriaga *et al.*, 1982; Verghese *et al.*, 1982; Abed *et al.*, 2000). Since their introduction in (Perez-Arriaga *et al.*, 1982; Verghese *et al.*, 1982), participation factors have been used for analysis, order reduction and controller design in a variety of fields, especially electric power systems. [1]

Next, a brief summary of modal participation factors is given, along with a derivation of input-to-state modal participation factors.

2.1 Modal participation factors

Consider a general continuous-time linear time-invariant system

$$\dot{x} = Ax(t) \tag{1}$$

where $x \in \Re^n$, and A is a real $n \times n$ matrix. Suppose that A has a set of n distinct eigenvalues $(\lambda_1, \lambda_2, \ldots, \lambda_n)$. Let $(r^1, r^2, \ldots, r^n)$ denote the right eigenvectors and $(l^1, l^2, \ldots, l^n)$ denote left (row) eigenvectors of the matrix A associated with the eigenvalues $(\lambda_1, \lambda_2, \ldots, \lambda_n)$, respectively.

The right and left eigenvectors are taken to satisfy the normalization

$$l^i r^j = \delta_{ij}$$

where δ_{ij} is the Kronecker delta:

$$\delta_{ij} = \begin{cases} 1 & i = j \\ 0 & i \neq j \end{cases}$$

The participation factor of the i-th mode in the k-th state is defined to be the complex number

$$p_{ki} := l_k^i r_k^i.$$

This formula also gives the participation of the k-th state in the i-th mode.

2.2 Input-to-state participation factors

The concept of participation factors of modes in states and vice versa has been extended to linear time invariant systems with inputs (Yaghoobi and Abed, 1999)

$$\dot{x} = Ax + Bu \tag{2}$$

$$y = Cx. \tag{3}$$

We consider the case where the input is applied to one component, say the q-th component, of the right side of (2) and only one state, say the k-th state, is measured. That is, in Eqs. (2)-(3), B and C take the form

$$\begin{aligned} B = e^q &= [0 \ \ldots \ 0 \ \underbrace{1}_{q-th} \ 0 \ldots 0]^T, \\ C = (e^k)^T &= [0 \ \ldots \ 0 \ \underbrace{1}_{k-th} \ 0 \ldots 0]. \end{aligned} \tag{4}$$

With this choice of C and B, in steady state the output in (3) (in the frequency domain) is given by

$$\begin{aligned} y(s) = x_k(s) &= C(sI - A)^{-1}Bu \\ &= \sum_{i=1}^{n} \frac{Cr^i l^i B}{s - \lambda_i} u(s) = \sum_{i=1}^{n} \frac{r_k^i l_q^i}{s - \lambda_i} u(s) \end{aligned} \tag{5}$$

We take

$$p_{qk}^i := |Cr^i l^i B| = |r_k^i l_q^i| \tag{6}$$

as *the participation factor of mode i in state k when the input is applied to state q*. We call this quantity the *input-to-state participation factor (ISPF)* for mode i, with measurement at state k and input applied to state q. Note that the ISPF is dimensionless given that the input and output vectors B and C take the special form in (4).

3. PRECURSOR-BASED MONITORING

The approach to instability monitoring presented here involves injecting probe signals at certain locations in a power network and monitoring the effects on measured output variables. Input-to-state participation factors introduced in this paper, play an important role in selection of sites for probe signal injection and output measurement.

As noted in (Hauer and Beshir, 2000), the recurring problems of system oscillations and voltage collapse are due in part to system behavior not well captured by the models used in planning and operation studies. In the face of component failures, system models become mismatched to the physical network, and are only accurate if they are updated using a powerful and accurate failure detection system. Therefore, it is important to

[1] In (Abed *et al.*, 2000), a new approach to defining modal participation factors was presented. The new approach involved taking an average or a probabilistic expectation of a quantitative measure of relative modal participation over an uncertain initial state vector. The new definitions were shown to reduce to the original definition of participation factors if the initial state obeys a symmetry condition.

employ nonparametric techniques for instability monitoring. In this work, noisy probe signals are used to help detect impending loss of stability.

Recently, monitoring systems for detecting impending instability in nonlinear systems were developed in (Kim and Abed, 2000). The work builds on Wiesenfeld's research on "noisy precursors of bifurcations," which were originally introduced to characterize and employ the noise amplification properties of nonlinear systems near various types of bifurcations (Wiesenfeld, 1985*a*; Wiesenfeld, 1985*b*). Noisy precursors are features of the power spectral density (PSD) of a measured output of a system excited by additive white Gaussian noise (AWGN). It was shown in (Kim and Abed, 2000) that systems driven by white noise and operating near an equilibrium point exhibit sharply growing peaks near certain frequencies as the system nears a bifurcation. In particular, it was shown that for the case of Hopf bifurcation (complex conjugate pair of eigenvalues crossing the imaginary axis transversely), the peak in the PSD occurs near ω_c, the critical frequency of the Hopf bifurcation.

In this work, we show that noisy precursors can be used as a warning signal indicating that the power system is operating dangerously close to instability. We also show that the spectrum of a measured state of the system is proportional to the square of the ISPFs. Thus, ISPFs can be used to determine the best location for applying the probe signal and for choosing which state to measure where the noisy precursor would be most apparent. Fig. 1 shows a schematic diagram of our instability monitoring technique.

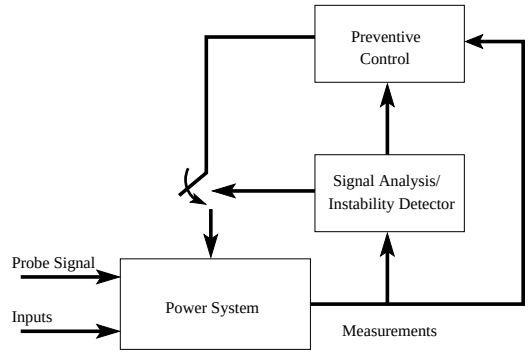

Fig. 1. Precursor-based instability monitor with external probe signal.

Consider a nonlinear dynamic system ("the plant")

$$\dot{x} = f(x, \mu) + \xi(t) \tag{7}$$

where $x \in R^n$, μ is a bifurcation parameter, and $\xi(t) \in R^n$ is a zero-mean vector white Gaussian noise process. Let the system possess an equilibrium point x_0. For small perturbations and noise, the dynamical behavior of the system can be described by the linearized system in the vicinity of the equilibrium point x_0. The linearized system corresponding to (7) with a small noise forcing $\xi(t)$ is given by

$$\dot{x} = Df(x_0, \mu)x + \xi(t) \tag{8}$$

where x now denotes $x - x_0$ (the state vector referred to x_0). For the results of the linearized analysis to have any bearing on the original nonlinear model, we must assume that the noise is of small amplitude.

We consider the case where the noise is applied to one state and the PSD of another state is calculated. That is, we consider the case where $\xi(t) = B\eta(t)$ with $B = e^q$, $\eta(t)$ is a scalar white Gaussian noise with zero mean and power σ^2, and the output is given by $y = Cx$ with $C = (e^p)^T$.

In steady state, the output of system (8) forced by a small AWGN is given by

$$\begin{aligned} y(s) = x_p(s) &= \sum_{i=1}^{n} \frac{Cr^i l^i B}{s - \lambda_i} \eta(s) \\ &= \sum_{i=1}^{n} \frac{r_p^i l_q^i}{s - \lambda_i} \eta(s). \end{aligned} \tag{9}$$

The PSD of the output of a linear system with transfer function $H(j\omega)$ is related to the PSD of the input by (Helstrom, 1991)

$$S_y(\omega) = H(j\omega)H(-j\omega)S_\eta(\omega) \tag{10}$$

Thus, the power spectrum of the p-th state is given by

$$\begin{aligned} S_{x_p} &= \left(\sum_{i=1}^{n} \frac{r_p^i l_q^i}{j\omega - \lambda_i} \right) \left(\sum_{k=1}^{n} \frac{r_p^k l_q^k}{-j\omega - \lambda_k} \right) \sigma^2 \\ &= \sigma^2 \sum_{i=1}^{n} \sum_{k=1}^{n} \frac{r_p^i l_q^i}{j\omega - \lambda_i} \ \frac{r_p^k l_q^k}{-j\omega - \lambda_k} \end{aligned} \tag{11}$$

Suppose that the system is nearing a Hopf bifurcation. Specifically, assume that a complex conjugate pair of eigenvalues is close to the imaginary axis, and has relatively small negative real part in absolute value compared to other system eigenvalues. Denote this pair as $\lambda_{1,2} = -\epsilon \pm j\omega_c$, with $\epsilon > 0$ small and $\omega_c > 0$:

$$|Re(\lambda_i)| \gg \epsilon, \quad i = 3, \ldots, n. \tag{12}$$

Under this assumption, $S_{x_p}(\omega)$ can be approximated as

$$\begin{aligned} S_{x_p}(\omega) \ &\approx \ \sigma^2 \sum_{i=1}^{2} \sum_{k=1}^{2} \frac{r_p^i l_q^i}{j\omega - \lambda_i} \ \frac{r_p^k l_q^k}{-j\omega - \lambda_k} \\ &= \ \sigma^2 \left(\frac{|r_p^1 l_q^1|^2}{\epsilon^2 + (\omega - \omega_c)^2} + \frac{|r_p^1 l_q^1|^2}{\epsilon^2 + (\omega + \omega_c)^2} \right. \\ &\quad \left. + \ 2\mathrm{Re} \left\{ \frac{1}{\epsilon + j(\omega - \omega_c)} \ \frac{(r_p^1 l_q^1)^2}{\epsilon - j(\omega + \omega_c)} \right\} \right). \end{aligned}$$

Here, r_p^i denotes the p-th component of the i-th right eigenvector r^i (the eigenvector corresponding to λ_i), and l_q^i denotes the q-th component of

the i-th left eigenvector l^i. Note that all terms containing λ_i, $i = 3, \ldots, n$ have been neglected and only terms containing the critical eigenvalues λ_1 and λ_2 have been retained. After algebraic manipulation and substituting $(r_p^1 l_q^1)^2 = \alpha + j\beta$ where $\alpha = |r_p^1 l_q^1|^2 \cos(2\theta_{pq})$ and $\beta = |r_p^1 l_q^1|^2 \sin(2\theta_{pq})$, with $\theta_{pq} = \tan^{-1}\left(\frac{Im\{r_p^1 l_q^1\}}{Re\{r_p^1 l_q^1\}}\right)$, the PSD of x_p can be rewritten as

$$\begin{aligned} S_{x_p}(\omega) &= \sigma^2 |r_p^1 l_q^1|^2 \left(\frac{1}{\epsilon^2 + (\omega - \omega_c)^2} + \frac{1}{\epsilon^2 + (\omega + \omega_c)^2} \right) \\ &\quad + \sigma^2 \frac{(\beta\epsilon + \alpha\omega_c)(\omega - \omega_c) + \epsilon(\epsilon\alpha - \omega_c\beta)}{(\epsilon^2 + \omega_c^2)(\epsilon^2 + (\omega - \omega_c)^2)} \\ &\quad - \sigma^2 \frac{(\beta\epsilon + \alpha\omega_c)(\omega + \omega_c) - \epsilon(\epsilon\alpha - \omega_c\beta)}{(\epsilon^2 + \omega_c^2)(\epsilon^2 + (\omega + \omega_c)^2)} \\ &= \sigma^2 |r_p^1 l_q^1|^2 \left[(1 + G_1(\omega)) \frac{1}{\epsilon^2 + (\omega - \omega_c)^2} \right. \\ &\quad \left. + (1 - G_2(\omega)) \frac{1}{\epsilon^2 + (\omega + \omega_c)^2} \right] \end{aligned} \quad (13)$$

where

$$\begin{aligned} G_1(\omega) &= \frac{1}{\epsilon^2 + \omega_c^2} \left[(\epsilon \sin(2\theta_{pq}) + \omega_c \cos(2\theta_{pq}))(\omega - \omega_c) \right. \\ &\quad \left. + \epsilon(\epsilon \cos(2\theta_{pq}) - \omega_c \sin(2\theta_{pq})) \right], \\ G_2(\omega) &= \frac{1}{\epsilon^2 + \omega_c^2} [(\epsilon \sin(2\theta_{pq}) + \omega_c \cos(2\theta_{pq}))(\omega + \omega_c) \\ &\quad - \epsilon(\epsilon \cos(2\theta_{pq}) - \omega_c \sin(2\theta_{pq}))]. \end{aligned}$$

For $\omega = \omega_c$ and sufficiently small ϵ ($\epsilon \ll \omega_c$), the power spectral density of x_p is given by

$$S_{x_p}(\omega) = \sigma^2 |r_p^1 l_q^1|^2 \left(\frac{1}{\epsilon^2} + O\left(\frac{1}{\epsilon}\right) + O(1) \right). \quad (14)$$

Note that the ISPFs are related to the PSD of the states of a system driven by small AWGN as in Eq. (13). The amplitude of the spectrum is proportional to the square of the ISPFs. The ISPFs can be used to determine the best location for applying the probe signal and also the state that will have the highest spectral peak.

4. INSTABILITY PROXIMITY INDEX

In this section, an instability proximity index that helps predict closeness to instability based on PSD measurements is given. Performance indices have been used to predict proximity to voltage collapse in power systems (PES, 2002). For example, stability indices based on sensitivity factors, singular values and eigenvalues have been used in the literature (PES, 2002).

In this paper, a sensitivity-based index is proposed. This index is based on online measurements of PSD peaks at certain critical frequencies. The proposed index is given by

$$PSDI = \frac{dPSD_x}{d\mu}. \quad (15)$$

Here, $PSDI$ is the power spectral density index, PSD_x is the power spectral density peak value at the critical frequency of the state x and μ is a bifurcation parameter of the system of interest. The instability index is calculated for the state x which has the highest ISPFs. This index grows significantly as the system approaches criticality, where it is theoretically infinity at criticality. The reciprocal of the index in more informative than the index itself as the reciprocal value approaches zero as the system approaches criticality. This index can be used to assist a system operator in taking a preventive action. For example, a threshold can be used such that if the index drops below that threshold, a preventive action is triggered.

5. CASE STUDIES

Below, the instability monitoring technique presented above is demonstrated on sample power system models. First, a single generator with an infinite bus together with excitation control is considered. Then, a three-generator nine-bus power system model is considered.

5.1 Single generator connected to an infinite bus

Consider a synchronous machine with excitation control connected to an infinite bus (Abed and Varaiya, 1984):

$$\begin{aligned} \dot{\delta} &= \omega \\ 2H\dot{\omega} &= -D\omega + \omega_0(P_m - P_e) \\ \tau'_{d0}\dot{E}'_q &= E_{FD} - E'_q - (X_d - X'_d)i_d \\ \tau_E\dot{E}_{FD} &= -K_E E_{FD} + V_R - E_{FD}S_E(E_{FD}) \\ \tau_F\dot{V}_3 &= -V_3 + \frac{K_F}{\tau_E}(-K_E E_{FD} + V_R - E_{FD}S_E(E_{FD})) \\ \tau_A\dot{V}_R &= -V_R + K_A(V_{REF} - V_t - V_3). \end{aligned}$$

It was shown that this system undergoes a Hopf bifurcation as the control gain in the excitation system K_A is increased beyond a critical value of 193.74. Details on the model and the parameters can be found in (Abed and Varaiya, 1984).

Next, we consider the system operating before the Hopf bifurcation, say at $K_A = 185$. The corresponding operating point is given by $x^0 = [1.3515,\ 0,\ 1.1039,\ 2.3150,\ 0,\ 0.5472]$. The eigenvalues of the Jacobian of the system evaluated at x^0 are $\{-0.0139 \pm j7.7707,\ -4.5832 \pm j12.6178, -2.1029 \pm j0.9417\}$.

Note that for this model, there are two physically feasible locations for applying the probe signal. The probe signal can be either applied to V_{ref} or to P_m. The ISPFs are used to determine the best location for applying the probe signal and which state to monitor. From the values of the

ISPFs (see Table 5.1), it is clear that mode 1 has higher participation in other states when the probe signal is applied to P_m than when applied to V_{ref}. This can also be seen from the PSDs shown in Figs. 2 and 3. Fig. 4 shows the PSDI based on measurements from the state V_R versus the exciter gain K_A.

5.2 Three-generator nine-bus power system

Below, we consider the Western System Coordinating Council (WSCC) 3-machine, 9-bus power system model, which is widely used in the literature (Sauer and Pai, 1998, pp. 170–177), (Milano, 2004). The dynamics of this model includes three

Table 1. ISPFs for the single generator power system model (partial listing).

States measured	Noise added to P_m	Noise added to V_{ref}
δ	$p^1_{21} = 0.0648$	$p^1_{61} = 0.0024$
ω	$p^1_{22} = 0.4923$	$p^1_{62} = 0.0185$
E'_q	$p^1_{23} = 0.0038$	$p^1_{63} = 0.0001$
E_{FD}	$p^1_{24} = 0.2084$	$p^1_{64} = 0.0078$
V_3	$p^1_{25} = 0.0068$	$p^1_{65} = 0.0003$
V_R	$p^1_{26} = 0.8006$	$p^1_{66} = 0.0301$

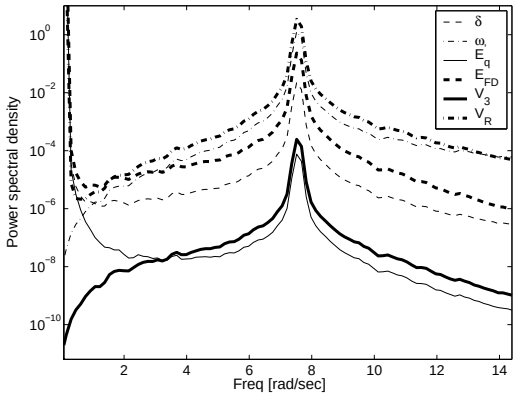

Fig. 2. PSDs of the states of the single generator power system model. The bifurcation parameter was set to $K_A = 185$. A zero mean and $(0.000032)^2$ power AWGN was added to P_m.

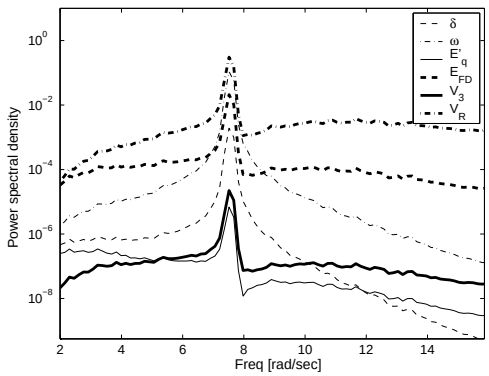

Fig. 3. PSDs of the states of the single generator power system model. The bifurcation parameter was set to $K_A = 185$. A zero mean and $(0.000032)^2$ power AWGN was added to V_{ref}.

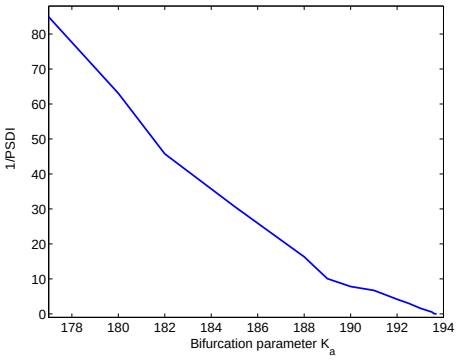

Fig. 4. Plot of the inverse of the PSDI of ω versus the bifurcation parameter K_A.

Table 2. Input-to-state participation factors for the 3-machine nine-bus system (partial listing). The load at bus 5 is 4.4 pu.

Noise added to	States measured E_{fd_1}	E_{fd_2}	E_{fd_3}
P_{m_1}	3.0017	2.6973	2.1357
P_{m_2}	2.6113	2.3465	1.858
P_{m_3}	4.7816	4.2967	3.4022
V_{ref_1}	0.0155	0.014	0.0111
V_{ref_2}	0.0233	0.021	0.0166
V_{ref_3}	0.0475	0.0427	0.0338

identical IEEE-Type I exciters for the three machines. The machine data and the exciter data are given in (Sauer and Pai, 1998; Milano, 2004).

In this model, a subcritical Hopf bifurcation occurs as the load on bus 5 is increased beyond 4.5 pu (Sauer and Pai, 1998). Our goal in this case study is to detect this impending loss of stability by using an AWGN probe signal and continuously monitoring the PSDs of certain states. This would give the system operator (or an automatic controller) valuable time to take appropriate preventive measures (e.g., shedding loads at certain buses). The simulations of this model were conducted using PSAT (Milano, 2004). For values of the load on bus 5 close to 4.0 pu, the linearization of the system at the operating point has two complex conjugate pair of eigenvalues close to the imaginary axis, $\lambda_{1,2} = -0.17665 \pm j8.184$ and $\lambda_{3,4} = -0.3134 \pm j1.7197$. As the load on bus 5 is increased further, the pair $\lambda_{3,4}$ approaches the imaginary axis, while the other pair $\lambda_{1,2}$ changes only slightly. For example, when the load at bus 5 is 4.4 pu, $\lambda_{1,2} = -0.18231 \pm j8.0978$ and $\lambda_{3,4} = -0.04602 \pm j2.1151$. Increasing the load on bus 5 beyond 4.5 pu causes the pair $\lambda_{3,4}$ to cross the imaginary axis from left to right.

From the values of the ISPFs calculated for this system, we found that both of the critical modes have higher participation when the probe signal is applied to P_{m_3}, the mechanical power of generator number 3. Also, we found that these modes have high participation in the field voltage of the exciters. Therefore, in the following simulations,

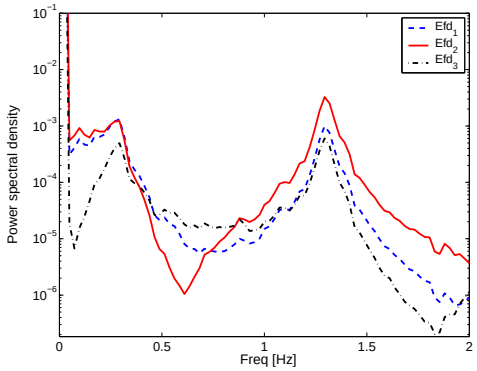

Fig. 5. PSDs of the states E_{fd_1}, E_{fd_2} and E_{fd_3}. The load on bus 5 was set to 4.0 pu. A zero mean and 0.05 power AWGN was added to P_{m_3}.

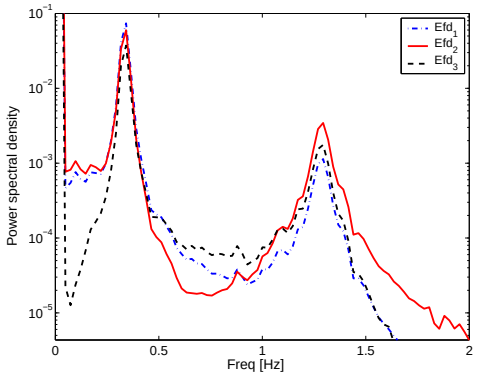

Fig. 6. PSDs of the states E_{fd_1}, E_{fd_2} and E_{fd_3}. The load on bus 5 was set to 4.4 pu. A zero mean and 0.05 power AWGN was added to P_{m_3}.

the probe signal is added to P_{m_3} and the power spectral densities of the field voltages of the three exciters (i.e., $E_{fd_i}, i = 1, 2, 3$) are monitored. Figs. 5 and 6 show the PSDs of E_{fd_i}, $i = 1, 2, 3$ when the load on bus 5 (P_{L_5}) is 4.0 pu and 4.4 pu, respectively. It is clear from Fig. 5 that when the load on bus 5 is 4.0 pu, the spectrum has two peaks at 0.28 Hz and 1.3 Hz. These two frequencies correspond to the complex eigenvalues $\lambda_{3,4}$ and $\lambda_{1,2}$, respectively. Note that the peak at 1.3 Hz that corresponds to the pair of complex eigenvalues $\lambda_{1,2}$ is higher than the peak at 0.28 Hz. However, when the load at bus 5 is increased to 4.4 pu, the peak at 0.28 Hz becomes much larger than the one at 1.3 Hz (see Fig. 6), which is an indicator that an instability is being approached. Fig. 7 shows the PSD of E_{fd_1} for three values of P_{L_5}: 4.0 pu, 4.25 pu and 4.4 pu.

ACKNOWLEDGEMENT

This research was supported in part by the National Science Foundation under Grants ECS-01-15160 and ANI-02-19162.

REFERENCES

Abed, E. H. and P. P. Varaiya (1984). Nonlinear oscillations in power-systems. *Int. Journal of Elec. Power & Energy Sys.* **6**(1), 37–43.

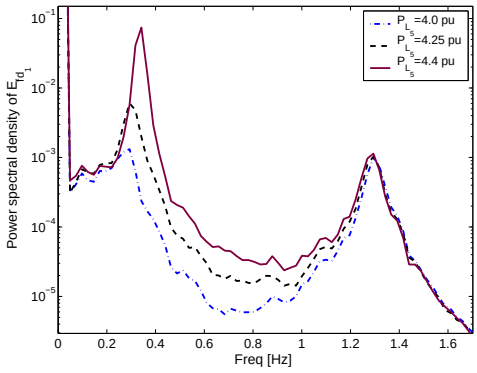

Fig. 7. Power spectral density of E_{fd_1} for three values of P_{L_5} (the load on bus 5). A zero mean and 0.05 power AWGN was added to P_{m_3}.

Abed, E. H., D. Lindsay and W. A. Hashlamoun (2000). On participation factors for linear systems. *Automatica* **36**, 1489–1496.

Hauer, J. F. and M. J. Beshir (2000). Dynamic performance validation in the western power system. In: *Association of Power Exchanges*. Kananaskis, Alberta.

Helstrom, C. W. (1991). *Probability and Stochastic Processes for Engineers*. second edition. Macmillan.

Kim, T. and E. H. Abed (2000). Closed-loop monitoring systems for detecting impending instability. *IEEE Trans. Circuits and Systems–I* **47**(10), 1479–1493.

Milano, F. (2004). *Power System Analysis Toolbox Documentation for PSAT*. Available online at http://www.power.uwaterloo.ca/˜fmilano/.

Perez-Arriaga, I. J., G. C. Verghese and F. C. Schweppe (1982). Selective modal analysis with applications to electric power systems, Part I: Heuristic introduction. *IEEE Trans. Power Appar. & Sys.* **101**(9), 3117–3125.

PES (2002). Voltage stability assessment: Concepts, practices and tools. IEEE Technical Report, number SP101PSS.

Sauer, P. W. and M. P. Pai (1998). *Power System Dynamics and Stability*. Prentice Hall. NJ.

van Cutsem, T. (2000). Voltage instability: Phenomena, countermeasures, and analysis methods. *Proc. IEEE* **88**(2), 208–227.

Verghese, G. C., I. J. Perez-Arriaga and F. C. Schweppe (1982). Selective modal analysis with applications to elec. power systems, Part II: Dynamic stability problem. *IEEE Trans. Power App. & Sys.* **101**(9), 3126–3134.

Wiesenfeld, K. (1985*a*). Noisy precursors of nonlinear instabilities. *J. Statistical Physics*.

Wiesenfeld, K. (1985*b*). Virtual Hopf phenomenon: A new precursor of period doubling bifurcations. *Physical Review A*.

Yaghoobi, H. and E.H. Abed (1999). Optimal actuator and sensor placement for modal and stability monitoring. In: *Proc. Amer. Control Conference*. San Diego, CA. pp. 3702–3707.